CONF-800502--5

# ANALYSIS OF A TRANSIENT LOAD MEASURING SYSTEM

MASTER

R. R. Good
EG&G Idaho, Inc.
P. O. Box 1625
Idaho Falls, ID 83415

T. R. Meachum
EG&G Idaho, Inc.
P.O. Box 1625
Idaho Falls, ID 83415

## ABSTRACT

An analysis of the performance of a load measuring system is presented. The load system was designed to measure the weight of a pressure vessel containing high pressure and temperature water. The uncertainty and frequency response of the system are quantified for both steady state and dynamic conditions as is the repeatability of the test rig. Computation of the mass flow exiting the system during explosive decompression of the system is also presented.

## SUMMARY

An analysis of the weight measuring system used in a series of transient steam water flow tests is presented. The analysis yields two sigma static uncertainties of 0.59% RG and dynamic uncertainties of 7.8% RG. The system frequency response is flat to 0.3 Hz, and was not quantified at any higher frequencies. The purpose of the weight measuring system is to provide a reference mass flow for assessing the performance of a variety of experimental mass flow transducers. Thus, in addition to the uncertainty in system weight, this analysis quantifies the repeatability of the test rig, and describes in detail the computation of mass flow given the time history of system weight.

## INTRODUCTION

The ability to accurately and repeatedly calibrate multiphase mass flow instrumentation is becoming increasingly important to the study of reactor safety. Questions that are of current prominence in the reactor safety field involve predicting and measuring fluid conditions within a reactor system during transients associated with hypothetical accidents. Chief of these hypothetical accidents are pipe ruptures which result in the abrupt decompression of the reactor system. The decompression results in multiphase (steam-water) flows occurring throughout the reactor system. The Loss-of-Fluid Test (LOFT) facility (1) was designed to conduct reactor transient tests. The data from the LOFT tests are used to verify and improve computer codes used for predicting such transients. LOFT uses several different methods for measuring fluid velocity and mass flux, of which the primary method to date has been a drag disc turbine (DDT).

One of the problems which has plagued the DDT, and indeed all other mass flow instrumentation, has been the lack of a full scale transient calibration facility. Such a facility is required to accurately reproduce the flow fields present at LOFT measurement stations during reactor transients. The full scale feature of the facility allows exact duplication of upstream piping geometry thus assuring equivalent flow fields between LOFT and the calibration facility. To meet the need of a full scale transient calibration facility, EG&G Idaho, Inc. had Wyle Laboratories construct a test facility capable of duplicating LOFT fluid conditions during decompression transients. This facility, the Wyle Transient Calibration Facility (WTCF) (2), was constructed with funds jointly provided by the Nuclear Regulatory Commission (NRC) and the Department of Energy (DOE).

The term calibration facility implies a reference for calibration exists. Unfortunately, no industry-wide standard exists for transient two-phase flow. The requirements for an acceptable reference were severe. The reference had to be impervious to the fluid conditions (15.5 MPa and 555 K), and produce an accurate estimate of the total mass flow regardless of the multiphase nature of the flow. These requirements were met by a load cell based weighing system. This paper presents an analysis of the frequency response, static and dynamic uncertainties of the load cell system.

The quantification of the uncertainty in mass flow measurement was achieved through a combination of experimental and analytical techniques. The lack of a recognized standard for multiphase mass flow calibration forces all uncertainty estimates to be compared to single-phase standards, this creates uncertainties quantifiable only by engineering judgement. The stochastic nature of fluid requires that averaging techniques be applied to the data to produce repeatable results. The selection of appropriate averaging methods also requires engineering judgement. Thus, the assessment of the accuracy of the reference instrumentation was a combination of engineering judgement and standard single-phase calibration techniques.

Uncertainty was quantified both for static and dynamic conditions. The static uncertainty limits the uncertainty in the total mass flow and provides a lower bound for the dynamic uncertainty if no filtering is applied. The dynamic uncertainty quantifies the frequency response of the mass flow measurement and the uncertainty in the measurement at each frequency. The mass measurement repeatability between tests is addressed both in the static and dynamic analyses.

## WEIGH SYSTEM DESCRIPTION

The design goal of the WTCF load cell weigh system was to weigh the WTCF system during explosive decompression (blowdowns). The weigh system comprised two primary subsystems: the load system and the data processing system. The load system produced a filtered electrical output proportional to the system weight. The data processing system used the electrical output of the load system to produce system weight and rate of change of system weight in engineering units. Figures 1 and 2 respectively present schematic representations of the weight and data processing subsystems.

The pertinent aspects of the load system are the load cells, the sway bracing, and the air bag supports for the blowdown piping. The design concept was to support the weight of the blowdown vessel and fluid on the load cells and the weight of the blowdown piping and stabilizing mass on the air bag support system. A finite element analysis, Reference 3, indicated that a negligible (< 15 kg) amount of load sharing would occur between the load cells and the air bag support. Unfortunately this analysis neglected long-term thermal effects as initially only short duration blowdowns were anticipated. The long-term thermal effects problem resulted in a redesign of the load cell system. The primary change was the addition of another load cell. The weigh system configuration change and its effect on overall system uncertainty will be documented in a later report. This report addresses only fast transients (< 300 s) for which the computer analysis was assumed valid.

The load cells, manufactured by Interface, were selected with fast transient capability. Each load cell has a range of 0 to 226.82 kN and a frequency response of not less than 100 Hz. The load cells were a strain gauge shear web design. Each load cell had a dual bridge; one was connected to the data acquisition system, and the other was displayed in real time. The system consisted of three load cells spaced at 120 degree intervals around the vessel as shown in Figure 3. The output of the load cells was algebraically summed which produced an output directly proportional to load.

The air bag support system was the only other major load bearing component in the weight system. The air bag support system consisted of two separate supports, one located next to the vessel, and one at the end of the blowdown leg. Air bags were supplied by Firestone and Lord Kinematic. Firestone air bags were located closest to the vessel and the Lord Kinematic air bags supported the stabilizing mass at the end of the blowdown leg. The relative stiffness of the air bag and load cell supports determined the amount of load sharing which occurred. The ratio of stiffness of load cells to air bag (see Reference 2) support was at least 1000; thus, the load cell support system would acquire at least 1000 N of load for every 1 N the air bag system acquired. The load sharing described assumes no major structural changes occurred in the system.

The only major nonvertical load bearing components of the weigh system were the sway braces. The design goal of the sway brace system was to restrain all horizontal motion of the vessel. The design concept was to restrain the vessel with large mechanical braces. Implementation of this system resulted in the sway braces absorbing some of the vertical loading of the vessel. This system was redesigned for the second series of tests.

## STATIC LOAD CALIBRATION

The WTCF load system was statically calibrated. The static load tests consisted of a series of fill, hydrostatic, and heatup tests. The fill tests established the accuracy of the load cells, the degree of load sharing between the load cells and air bag supports, and the effects of asymmetric loads on the vessel. The hydrostatic pressure tests and heatup tests quantified the WTCF system sensitivity to pressure and temperature. The fill tests were conducted prior to and during the actual blowdown testing period. The pressure sensitivity of the weigh system was not suspected until after testing began; thus the pressure tests were conducted during the transient testing period. Attempts at quantifying the temperature sensitivity were made prior to and during transient testing. The results of the static load testing were, in general, satisfactory.

The fill tests consisted of metering water into the WTCF system and recording the output of the load cells. A total of six cold fil tests were conducted on the WTCF system. The tests spanned a 2 1/2-month interval. Table I summarizes the data from these tests and Figure 4 is a plot of a typical series of data sets. The reference instrument for each fill test was a Foxboro Mark 1 F1-16-S8 full-flow turbine. The uncertainty of this turbine was <0.2% RG as determined by single-phase flow testing by the Foxboro Company. The data used to calculate the WTCF system static uncertainty were acquired by the Wyle computer system, and therefore incorporated the uncertainties due to quantization, signal transmission, and computer system effects.

The effect of asymmetric system loading was quantified during the fill tests and by subjecting the load ring to point loads of approximately 1250 N. Asymmetric loads of approximately 4406 N were placed on the system during the fill tests due to the mass distributed in the blowdown piping. No measurable change in the sum of the load cell outputs was detected while asymmetric loads were

placed on the system; therefore, the effect of asymmetric loads on system uncertainty was deemed negligible, <0.05% RG.

The WTCF system static load uncertainty design requirement was 1% RG and the range was 40800 N. Range was determined by the mass of water required to fill the WTCF system at 15.5 MPa and 550 K. The required uncertainty of the weigh system was achieved after modification of the air regulating system and the turbine meter fill system. The static system weigh uncertainty was 0.59% RG (241 N).

The long-term drift uncertainty of the weigh system was established by repeating the calibrated fill tests approximately two months later. Figure 5 is a comparison of two calibration tests taken two months apart. There is no statistically significant (95% confidence) difference in the calibration coefficient (the offset varies, but this is removed on a test by test basis). Thus, long-term drift uncertainty is deemed negligible (<0.05% RG).

Uncertainty in system load due to pressure effects was quantified in a series of cold and hot hydrostatic tests. The results of these tests are tabulated in Table II. Figures 6 and 7 represent the range of results obtained. A total of four cold pressure tests and two hot pressure tests were conducted. In general, the system load appeared sensitive to pressure; however, no repeatable functional relationship could be derived. Investigation of system load at decompression initiation revealed a step change in load occurring simultaneously with system subcooled depressurization to saturation and no detectable load sensitivity to pressure during the remaining depressurization. Figure 8 is a typical load cell blowdown trace illustrating the initial step change. Analysis of data gathered during transient testing indicated that the sway brace system was assuming significant vertical load during system pressurization and was releasing that load when the depressurization shock wave propagated through the system. A hot hydrostatic test and system depressurization were conducted with the sway brace system removed to verify the analysis. Figure 9 presents the data from the hot hydrostatic test with sway brace removed. The data indicate a slight increase in load with pressure. The increase in system load was commensurate with the mass required to raise the system pressure by 7.5 MPa. Thus, the removal of sway braces removed any system pressure sensitivity. The weigh system uncertainty due to pressure changes was deemed negligible (<0.05%) if a mechanical shock sufficient to remove any friction vertical load bearing in the sway brace system occurred prior to measurement. If a mechanical shock does not occur, the uncertainty is approximately 27% RG.

The weigh system uncertainty due to temperature fluctuations was not fully quantified. Tests were conducted to reveal system sensitivity to small (20 K) temperature fluctuations. Those tests demonstrated no significant weigh system temperature sensitivity. WTCF system design precluded varying system temperature significantly while maintaining system mass constant. Thus, no quantitative large-scale system temperature sensitivity was calculated. System temperature sensitivity was judged negligible.

The static weigh system uncertainty consists only of the uncertainty in the force measurement of the load cells as all other uncertanties are less than 0.05% RG, assuming that the effects of the sway bracing have been nullified. The uncertainty in system weight under static conditions is therefore $\pm$255 N ($\pm$25.5 kg or 0.59% RG).

## DYNAMIC LOAD UNCERTAINTY

The quantification of the WTCF system's dynamic uncertainty required both experimental and analytic methods. The experimental methods allowed the direct measurement of the system's response to physical excitation. The analytic approach yield estimates of the system uncertainty given the system's static response and the filtering applied to the output. Thus, estimates of the system's frequency response have been obtained experimentally, and quantification of the system uncertainty has been obtained analytically.

The experimental analyses involved the load cells and their structural support system. The support system acted as a complex damped spring mass system, the spring constants, etc., of which are unknown. The experiments performed to quantify the system frequency response included low frequency excitation of the system and broad band system excitation via explosive decompression of the system. The lowest frequency observed during either explosive decompression or low frequency excitation was 3 Hz. Figures 10 through 13 are power spectral densities (PSDs) of the individual load cells and their electronic summation. There is a clear peak evident in the PSDs of load cells 002 and 242, and a slightly more ill defined peak in load cell 122 and the net load. All of these peaks occur within 0.2 Hz of 3 Hz. Figures 14 and 15 present PSDs of the output of a velocity and momentum flux instrument, respectively. These instruments were located in the center of the blowdown piping 2 m from the blowdown vessel. Neither the velocity or momentum flux PSD exhibited any clearly defined peaks. Thus, since these two measurements incorporate both density and velocity measurements, it is evident that the 3-Hz phenomena measured by the load cell system was an artifact of the load cells and their support system, not a real oscillation in mass flow. The experimental data then provided the basis for engineering judgement in establishing the upper bound of frequency response for mass flow computed using the load cells. This upper bound was set at 0.3 Hz, one decade below the lowest measured load cell system resonant frequency.

The computational software system provided the means for extracting the desired frequency range and calculating the mass flow given system mass. Analysis of the software system provided an estimate of the uncertainty in mass flow after the signal had been processed. Signal processing

consisted of analog and digital filtering. The analog filtering consisted of a 4 pole, 10-Hz filter. The digital filter was a convolution of a 112 term low pass filter and a 25 term derivative filter. The digital filters were implemented as a weighted sum of finite differences. Figure 16 is the transfer function of the digital filter. All signals used to calculate the static uncertainties were passed through the analog filter, hence any uncertainty associated with the analog filter is integral to the static uncertainty estimate. Uncertainties associated with the digital filter were calculated using Equation (1) (see Reference 4).

$$\sigma_f^2 = \sigma_u^2 \sum_{K=-K}^{K} C_K^2 \qquad (1)$$

where:

$\sigma_f^2$ = uncertainty in filtered output

$\sigma_u^2$ = uncertainty in unfiltered output

$C_K$ = coefficients of digital filter.

Equation (1) yields an estimated uncertainty in mass flow of $2.16 \times 10^{-3}$ N/s (0.22 g/s) given the static uncertainty of 25.5 kg. A basic assumption of Equation (1) is that the system being filtered is a linear time invariant system. This assumption is probably invalid considering signal magnitudes of the order of 1 N or less. Thus, a reasonable engineering estimate of the uncertainty in system mass flow is 0.5 kg/s ($2\sigma$).

The dynamic uncertainty within any single test has now been analytically quantified. The dynamic repeatability however remains unknown. The dynamic repeatability is a function of many independent variables. These variables include initial system pressure, water temperature, metal temperature, and temperature distribution. Few of these parameters are well defined, thus an experimental approach must be employed to obtain meaningful estimates of the system's dynamic repeatability.

The WTCF experimental series included several replications of identical pretest configurations. Table III presents the results of comparing the first and second test series. Figure 17 is an overlay of the mass flow for three identical blowdown tests. Estimates of the instantaneous repeatability between tests were obtained by computing the deviation from the first test of the test series. All tests started at time zero as defined by the time a 5.0 MPa drop occurred across an orifice in the blowdown piping. Equation (2) was used to compute system instantaneous repeatability as well as integrated mass repeatability.

$$\sigma_I = \sqrt{\frac{\sum_{j=2}^{n} (X_1 - X_j)^2}{n-1}} \qquad (2)$$

where:

$X_1$ = reference channel

$X_j$ = all other channels

$\sigma_I$ = instantaneous standard deviation.

Figure 18 is a plot of instantaneous repeatability of mass flow for the first test series. System instantaneous repeatability varies widely during the blowdowns with the largest levels occurring during the subcooled portion of the blowdowns and at approximately 20 to 25 s. The mean instantaneous repeatability in mass flow for time segment is given in Table III-C.

## CONCLUSION

The transient steam-water calibration facility's reference mass flow system has proven to be an accurate, repeatable, and durable system. The isolation of the transducers from the internal environment of the system allowed the mass flow system to perform reliably for more than 20 experiments. The nature of the transducers, that they measure system weight directly, has contributed to their accuracy and has eased the computational requirements to produce mass flow rate. The uncertainty in static system weight is ±25.5 kg, the uncertainty in mass flow (assuming filtering is applied to the signal) is 0.5 kg/s. The weight system's frequency response is flat to 0.3 Hz and has not been quantified for greater frequencies. Additionally, the transient facility's repeatability has been quantified. The repeatability of the weigh system is an integral part of the transient system's repeatability, but has not been quantified separately. The transient system's worst case repeatability is ±20.1 kg/s, 7.8% of range.

It is the recommendation of the authors that load cell based systems be considered for all future transient two-phase systems and that weigh systems be recommended as a standard reference for the industry.

## REFERENCES


1. Reeder, D. L., LOFT System and Test Description (5.5 ft Nuclear Core 1 LOCEs), NUREG/CR-0247, TREE-1208, July 1978.

2. Wambach, Jacqui, et al., Wyle Transient Test EDR, February 1980.

3. Martinell, John, et al., "Performance Assessment of Mass Flow Rate Measurement Capabilities in the Large Scale Transient Two-Phase Flow Test System," 2nd Multiphase Flow and Heat Transfer Workshop, Miami, Florida, April 1979.

4. Hamming, R. W., Digital Filters, Prentice Hall, Inc., Englewood Cliffs, New Jersey, 1977.

TABLE I

Calibrated Fill Tests of the Wyle Transient Test Facility

| Test | Date | Calibration Coefficient kg/V* | Calibration Coefficient N/V | Correlation Coefficient | Standard Deviation of Y on X kg | Standard Deviation of Y on X N | Number of Points |
|---|---|---|---|---|---|---|---|
| 1 | 6/26/79 | 1731.6 | 17282 | 0.9997 | 23.7 | 237 | 21 |
| 2 | 6/28/79 | 1690.5 | 16871 | 1.0000 | 10.0 | 100 | 22 |
| 3 | 6/28/79 | 1689.5 | 16861 | 1.0000 | 12.7 | 127 | 19 |
| 4 | 7/2/79 | 1434.5** | 14316 | 1.0000 | 66.2 | 661 | 9 |
| 5 | 7/25/79 | 1699.5 | 16961 | 0.9999 | 8.8 | 88 | 27 |
| 6 | 8/29/79 | 1702.7 | 16993 | 1.0000 | 8.7 | 87 | 24 |

* Flowmeter partially bypassed, thus this point is not used in any analyses.

** Volts = sum of output of load cells 1, 2, and 3 from data acquisition system output.

TABLE II

Wyle Transient Test System Pressure Sensitivity

| Test | Pressure Range (MPa) | Maximum Force Range (N) | Date | Temperature (K) |
|---|---|---|---|---|
| 1 | 15 | 1355 | 8-6-79 | 350 |
| 2 | 14 | 9108 | 8-22-79 | 350 |
| 3 | 15 | 1014 | 8-28-79 | 350 |
| 4 | 5 | 3401 | 8-30-79 | 500 |
| 5 | 7.5 | 1181 | 9-5-79 | 500 |
| 6 | 17 | 1866 | 7-25-79 | 350 |

TABLE III

Comparison of Instanteous Repeatability

A. Root Mean Square Error (kg/s)

| Test Series | Time Interval (s) 0-10 | 10-20 | 20-25 | 25-40 | 40-60 |
|---|---|---|---|---|---|
| IA1 | 20.1 | 9.4 | 17.2 | 10.3 | 2.1 |
| IA2 | 22.8 | 7.4 | 16.6 | 5.0 | 1.9 |

B. Mass Flow (kg/s)

| Test Number | Time Interval (s) 0-10 | 10-20 | 20-25 | 25-40 | 40-60 |
|---|---|---|---|---|---|
| IA101 | 175.7 | 128.9 | 59.6 | 18.2 | 3.6 |
| IA102 | 188.0 | 126.3 | 83.7 | 28.5 | 2.6 |
| IA103 | 175.6 | 130.1 | 83.7 | 30.8 | 4.0 |
| IA1 Series (Average) | 179.8 | 128.4 | 75.7 | 25.8 | 3.4 |
| IA201 | 178.2 | 129.5 | 85.9 | 29.5 | 3.5 |
| IA202 | 169.4 | 130.3 | 74.2 | 24.9 | 2.6 |
| IA2 Series (Average) | 173.8 | 129.9 | 80.1 | 27.2 | 3.1 |

C. Percent of RD Uncertainty in Mass Flow

| Test Number | Time Interval (s) 0-10 | 10-20 | 20-25 | 25-40 | 40-60 |
|---|---|---|---|---|---|
| IA101 | 11 | 7 | 29 | 57 | 58 |
| IA102 | 11 | 7 | 21 | 36 | 81 |
| IA103 | 11 | 7 | 21 | 33 | 53 |
| IA1 Series (Average) | 11 | 7 | 23 | 40 | 62 |
| IA202 | 13 | 6 | 19 | 17 | 54 |
| IA203 | 13 | 6 | 22 | 20 | 73 |
| IA2 Series (Average) | 13 | 6 | 21 | 18 | 61 |
| Mean | 12 | 7 | 23 | 32 | 63 |

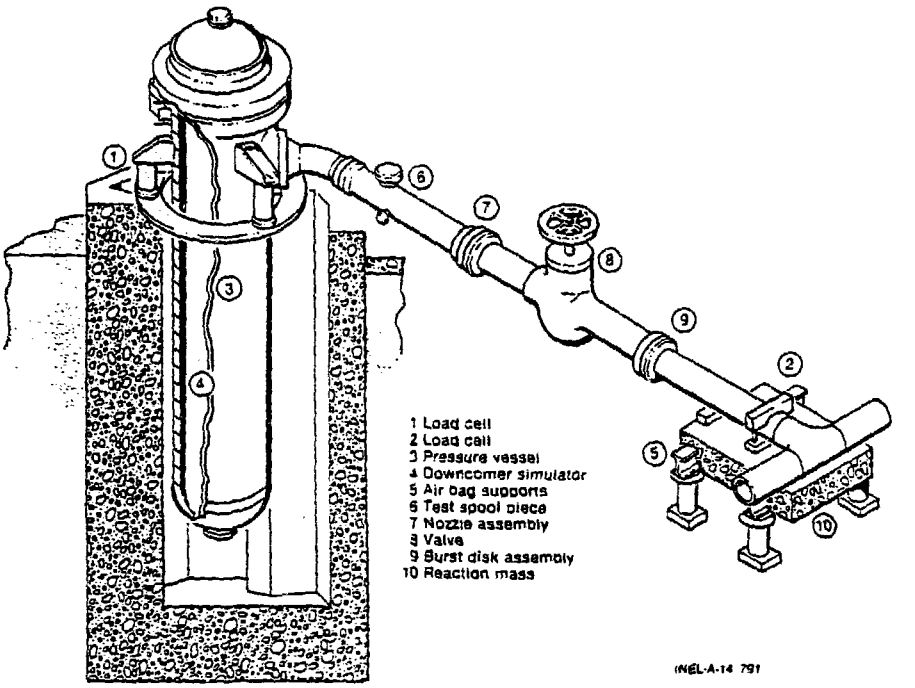


Figure 1. Schematic of Wyle transient test system.

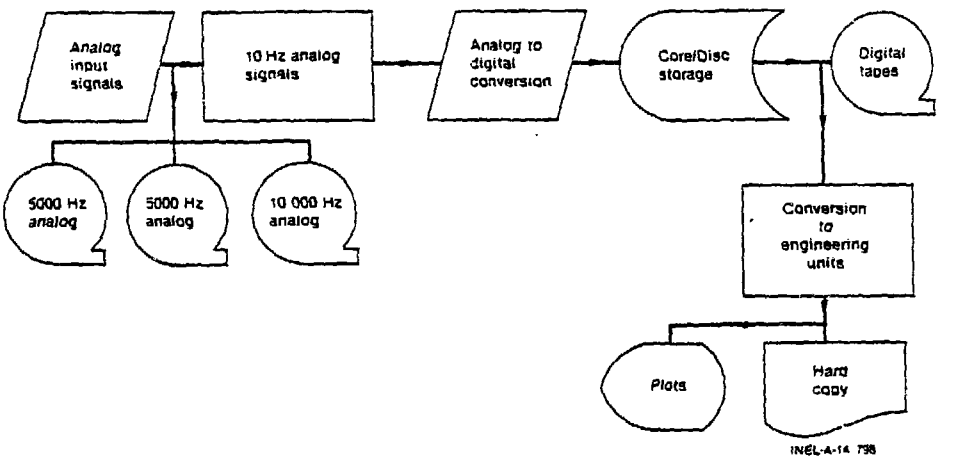


Figure 2. Wyle data processing subsystem.

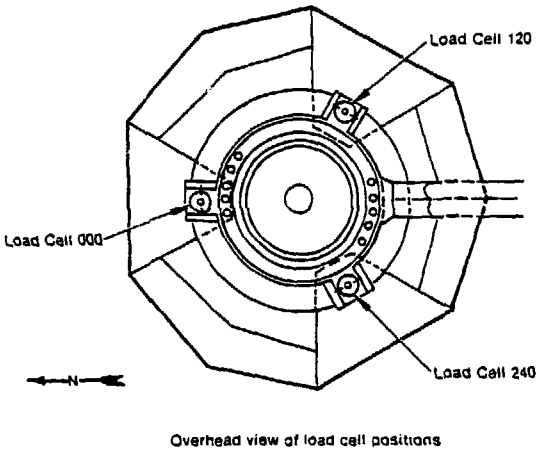


Figure 3. Overhead view of load cell positions.

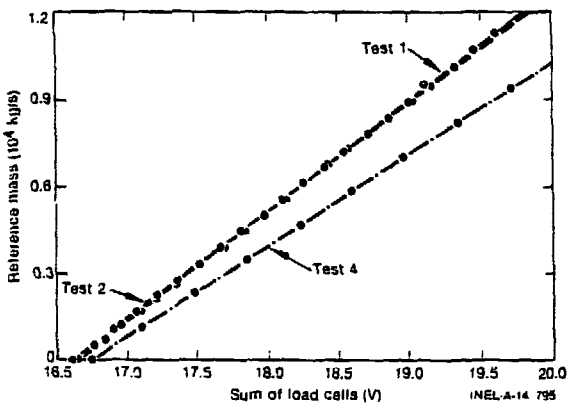


Figure 4. Wyle load cell calibration for Tests 1, 2, and 4.

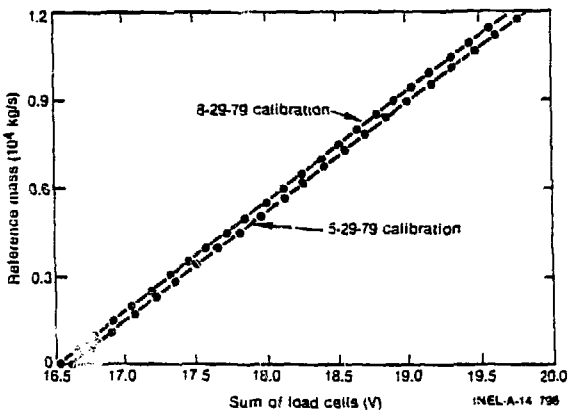


Figure 5. Wyle long-term drift tests.

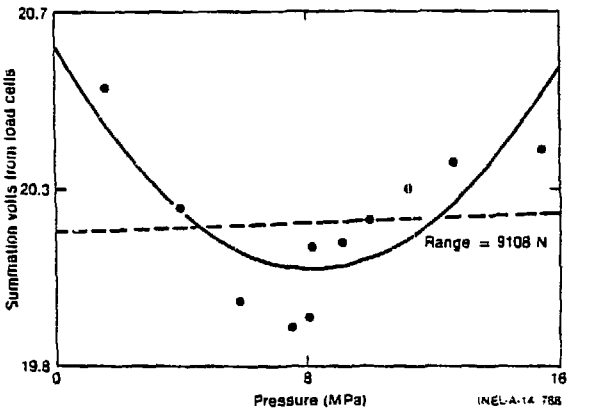


Figure 6. Wyle load cell pressure sensitivity (worst case).

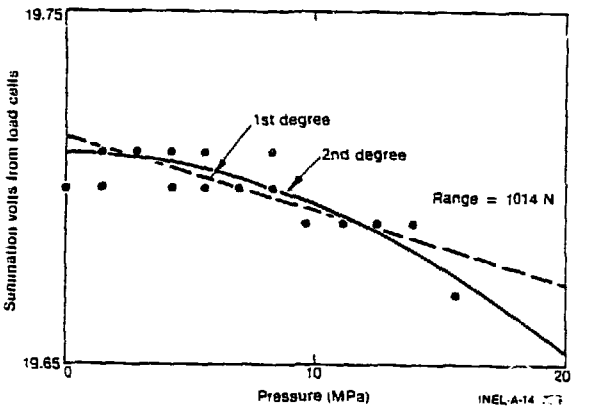


Figure 7. Wyle load cell pressure sensitivity (best case).

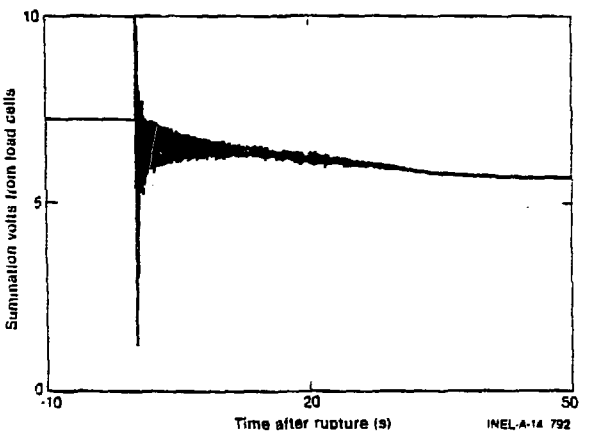


Figure 8. Typical load cell blowdown voltage trace.

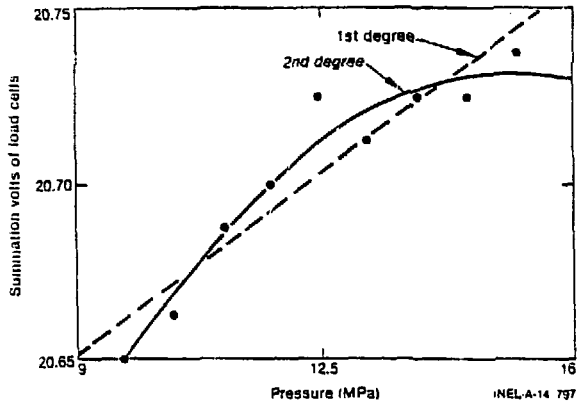


Figure 9. Wyle load cell pressure sensitivity test with sway brace removed.

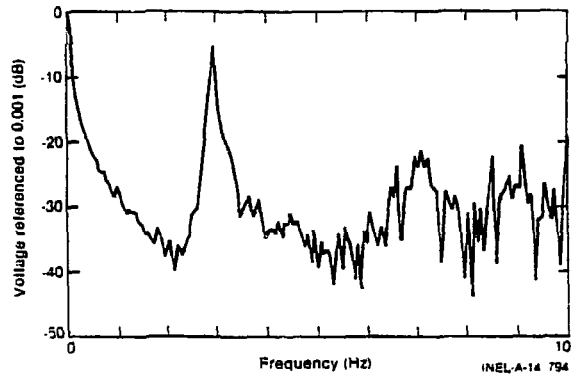


Figure 11. Power spectral density of LC-002, IA101, from +2 to +37 s. Sampling frequency = 32, Eq. filter frequency = 10, frame count = 2, APS accuracy = ±70.71%, input range = ±4 V, resolution = 0.0625 Hz/line.

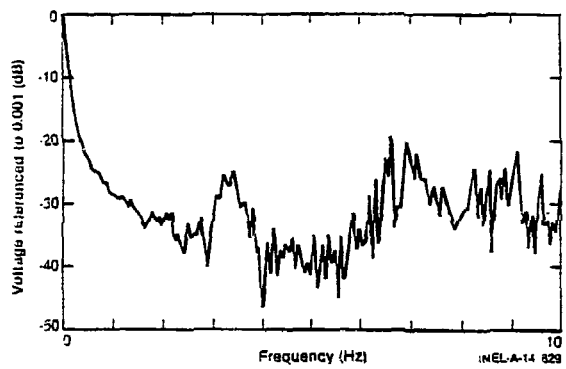


Figure 10. Power spectral density of LC-122, IA101, from +2 to +37 s. Sampling frequency = 32, Eq. filter frequency = 10, frame count = 2, APS accuracy = ±70.71%, input range = ±4 V, resolution = 0.0625 Hz/line.

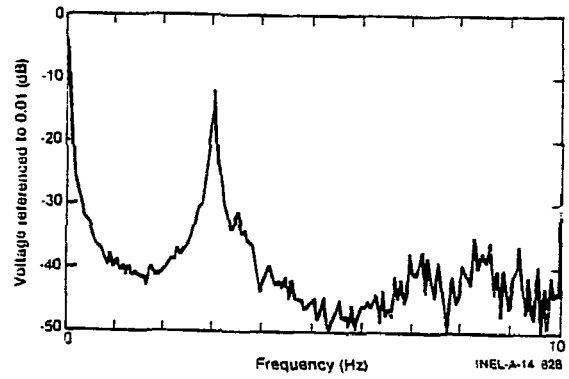


Figure 12. Power spectral density of LC-242, IA101, from +2 to +37 s. Sampling frequency = 32, Eq. filter frequency = 10, frame count = 2, APS accuracy = ±70.71%, input range = ±4 V, resolution = 0.0625 Hz/line.

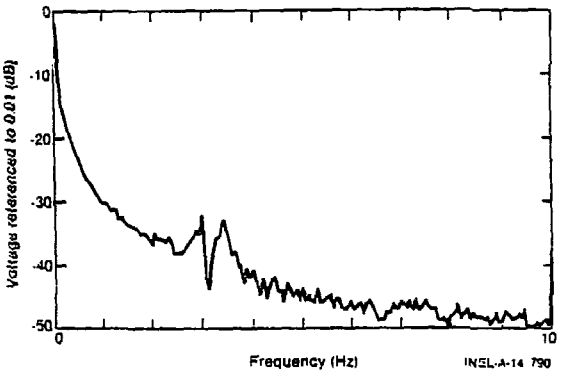


Figure 13. Power spectral density of net load, IA101, from +2 to +37 s. Sampling frequency = 32, Eq. filter frequency = 10, frame count = 2, APS accuracy = ±70.71%, input range = ±4 V, resolution = 0.0625 Hz/line.

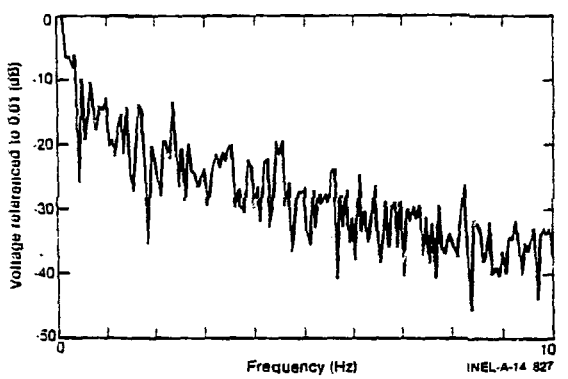


Figure 14. Power spectral density of turbine volts, IA101, from +2 to +37 s. Sampling frequency = 32, Eq. filter frequency = 10, frame count = 2, APS accuracy = ±70.71%, input range = ±4 V, resolution = 0.0625 Hz/line.

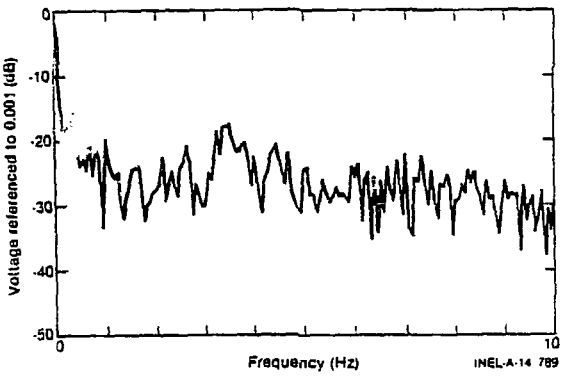


Figure 15. Power spectral density of drag disc volts, IA101, from +2 to +37 s. Sampling frequency = 32, Eq. filter frequency = 10, frame count = 2, APS accuracy = ±70.71%, input range = ±4 V, resolution = 0.0625 Hz/line.

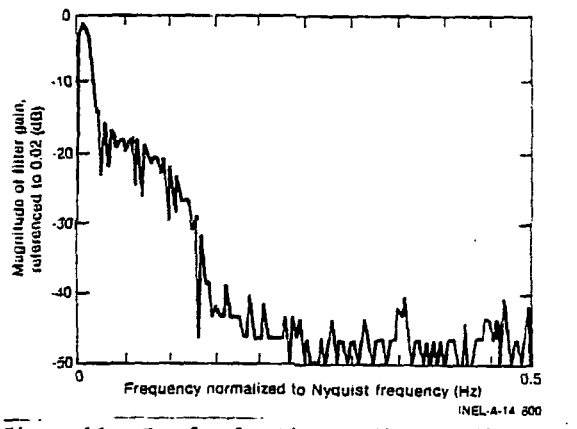


Figure 16. Tranfer function of digital filter.

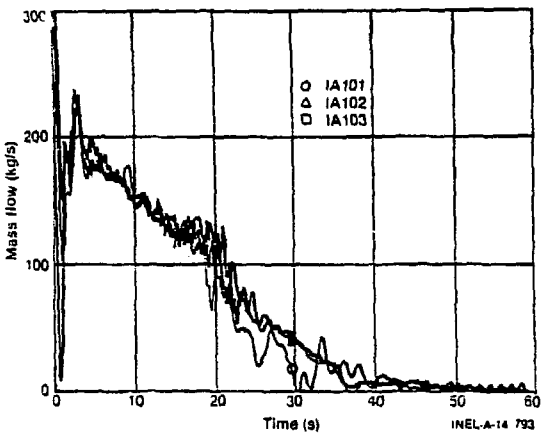


Figure 17. Overlay of Test Series IAi.

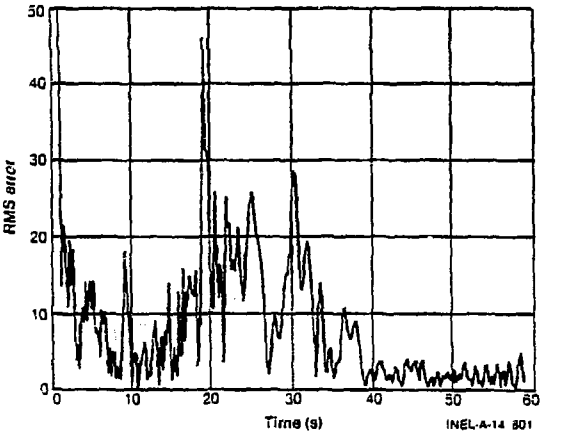


Figure 18. Instantaneous repeatability of IAl Test Series.